Doppler-Raman crossover in resonant scattering by a moving layer

A. V. Poshakinskiy,[1,*] A. N. Poddubny,[1] and N. A. Gippius[2]
[1]*Ioffe Institute, St. Petersburg 194021, Russia*
[2]*Skolkovo Institute of Science and Technology, Skolkovo 143025, Russia*

(Received 12 August 2020; accepted 30 September 2020; published 23 October 2020)

We consider theoretically light scattering by a resonant layer that periodically moves in real space. At small frequencies of motion the scattered light spectrum reveals the frequency shift that is governed by the Doppler effect. At higher motion frequencies, the scattered light spectra acquire sidebands stemming from the Raman effect. We investigate the crossover between these two regimes and propose a realistic quantum well structure for its observation.

DOI: 10.1103/PhysRevA.102.043523

I. INTRODUCTION

Frequency conversion is a basic nonlinear optical process, widely used for signal multiplexion and frequency comb generation [1]. An alternative approach is offered by optomechanical and optoacoustic nonlinearities [2–4]. The advantage of optomechanical systems is their relative compactness, enabling manipulation of the spectrum of classical and quantum light on the nanoscale [5,6]. Specifically, mechanical motion or deformation leads to a dynamical modification of optical properties such as refractive index [7], optical gain [8], and resonance frequency [9], allowing one to control the light intensity, frequency [10,11], and propagation direction [12], or induce synthetic magnetic [13] and spin-orbit [14,15] fields. The simplest example of motion-induced frequency conversion is given by the Doppler effect. The motion of the light source with respect to the observer with a constant velocity v leads to the shift of the observed light frequency by $(v/c)\omega_0$, where ω_0 is the emitter frequency and c is the speed of light. Another opportunity for frequency conversion is given by the Raman effect. When the optical properties of the medium oscillate at frequency Ω, the scattered light spectrum acquires sidebands shifted by Ω from the initial frequency. Both Doppler and Raman effects can be realized if one considers light scattering on an object periodically moving in space. While the two effects share the same origin, the corresponding frequency shifts are distinct. The Raman shift of the scattered light frequency is always a multiple of mechanical motion frequency Ω, while the Doppler frequency shift $(\Omega u_0/c)\omega_0$, being proportional to the motion velocity, scales linearly with the mechanical motion amplitude u_0. In this paper, we consider light scattered by a resonant layer oscillating in space. We calculate the scattered light spectra, identify the regimes where Doppler and Raman shifts can be observed, and investigate the crossover between them.

II. MODEL

We study light reflection and transmission through a moving layer with resonant polarizability. The microscopic origin of the resonant response might be the exciton resonance in semiconductors, plasmon resonance in metals, or atomic resonances (see Ref. [12] for a survey of resonant optomechanical systems). We suppose that the layer is a macroscopic system that can be described in the framework of classical electrodynamics. The light is incident along the layer normal z and linearly polarized along x (see Fig. 1). The layer motion along the z axis is characterized by the displacement $u_z(t)$. The system can be described by the action

$$S = \frac{1}{8\pi}\int \left[E_x^2(z,t) - B_y^2(z,t)\right]dz\,dt + \int P_x(t)\left\{E_x[u_z(t),t] + \frac{\dot{u}_z(t)}{c}B_y[u_z(t),t]\right\}dt + S_d, \tag{1}$$

where the dot denotes the time derivative. The first term in Eq. (1) is the action of a free electromagnetic field where the electric and magnetic fields can be expressed via the vector potential $A_x(z,t)$ as $E_x = -(1/c)(\partial A_x/\partial t)$ and $B_y = \partial A_x/\partial z$. The second term in Eq. (1) describes the interaction of the layer polarization $P_x(t)$ with the electromagnetic field (see the Appendix for the derivation). The last term S_d is the action describing layer polarization. We are interested in the layer with a resonant response, so we take the simplest model of a harmonic oscillator with the eigenfrequency ω_0, described by the Lagrangian

$$S_d = \frac{\pi}{2c\Gamma_0}\int\left\{\left(\frac{dP_x}{dt_0}\right)^2 - \omega_0^2 P_x^2\right\}dt_0. \tag{2}$$

Here, $dt_0 = dt\sqrt{1-\dot{u}_z^2(t)}$ is the time in the moving reference frame and the constant Γ_0 is the radiative decay rate of the oscillator, as justified below.

*poshakinskiy@mail.ioffe.ru

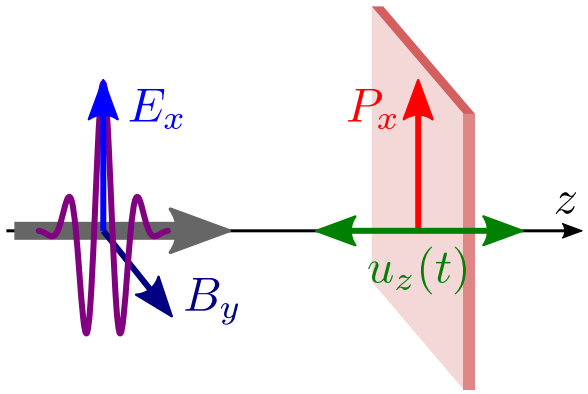

FIG. 1. A sketch of a short light pulse incident upon a layer periodically moving in space.

The action Eq. (1) yields the Euler-Lagrange dynamic equations

$$\frac{1}{c^2}\frac{\partial^2 A_x}{\partial t^2} - \frac{\partial A_x}{\partial z^2} = \frac{4\pi}{c}\frac{dP_x}{dt}\delta[z - u_z(t)], \tag{3}$$

$$\frac{d^2P_x}{dt_0^2} + 2\Gamma\frac{dP_x}{dt_0} + \omega_0^2 P_x = -\frac{\Gamma_0}{\pi}\frac{d}{dt_0}A_x[u_z(t), t], \tag{4}$$

where we introduced in Eq. (4) the oscillator damping with the rate Γ accounting for nonradiative decay processes. Equation (3) can be solved using the Green's function $G(z,t) = (c/2)\theta(ct - |z|)$ and yields

$$A_x(z,t) = A_x^{(0)}(z,t) + 2\pi P_x[t^*(z,t)], \tag{5}$$

where $A_x^{(0)}$ is the vector potential of the incident wave and $t^*(z,t) = t - |z - u_z[t^*(z,t)]|/c$. In particular, $t^*[u_z(t),t] = t$, so $A[u_z(t),t] = A_x^{(0)}[u_z(t),t] + 2\pi P_x(t)$. Substituting this into Eq. (4), we obtain a closed-form equation for the polarization,

$$\frac{d^2P_x}{dt_0^2} + 2\Gamma'\frac{dP_x}{dt_0} + \omega_0^2 P_x = -\frac{\Gamma_0}{\pi}\frac{d}{dt_0}A_x^{(0)}[u_z(t),t], \tag{6}$$

where $\Gamma' = \Gamma + \Gamma_0$. As follows from Eq. (6), the interaction of the layer polarization with the electromagnetic field leads to an increase of the polarization decay rate by Γ_0. Therefore, the latter describes the radiative decay rate of the oscillator.

III. TIME-RESOLVED SPECTROSCOPY

In order to reveal the frequency conversion for light reflected from the oscillating layer and analyze the crossover between the Doppler and Raman effects, we propose to use optical spectroscopy with a temporal resolution. In such an approach, which is an alternative to traditional frequency-resolved spectroscopy, one studies the response of the system to short optical pulses. When the probe pulse duration is smaller than the inverse width of the resonance, the reflected pulse spectrum matches the frequency dependence of the reflection coefficient [16–18]. Here, since the system under study changes with time, the reflected pulse spectrum depends on the time of incident pulse arrival and characterizes the system reflectivity at that moment. To map the evolution of optical properties, one should probe the system at moments corresponding to various phases of mechanical motion. The temporal separation between these moments should be kept sufficiently large to avoid the interference of different probe pulses.

We consider the illumination with a single δ pulse, described by the electric field

$$E^{(0)}(z,t) = \delta(t - \tau - z/c) \tag{7}$$

and vector potential $A^{(0)}(z,t) = -c\theta(t - \tau - z/c)$, where τ is the time of pulse arrival to $z = 0$. In what follows we suppose that (i) the mechanical frequency Ω is much smaller than the optical frequency ω_0, i.e., the Raman shift is small as compared to the light frequency. (ii) Motion is nonrelativistic, $\dot{u}_z \ll c$; then the Doppler shift $\omega_0\Omega u_0/c$ is also small as compared to the light frequency. These assumptions are valid for any solid-state optomechanical system [19]. Relativistic motion can only be achieved for, e.g., density waves in plasma [20], which are out of the scope of the present paper. If conditions (i) and (ii) are fulfilled, Eq. (6) is solved as

$$P_x(t) = -\frac{\Gamma_0}{\pi}\int \frac{e^{-i\omega[t-\tau-u_z(\tau)/c]}}{\omega^2 - \omega_0^2 + 2i\omega\Gamma'}\frac{d\omega}{2\pi}. \tag{8}$$

Substituting this result into Eq. (5), we obtain the vector potential of the reflected wave,

$$A_x^{(r)}(z,t) = \frac{2\Gamma_0}{\omega_0}\theta(\tau')\sin\omega_0\tau'\, e^{-\Gamma'\tau'}, \tag{9}$$

where $\tau' = t + z/c - \tau - [u_z(\tau) + u_z(t + z/c)]/c$. The reflected pulse spectrum, $E_x^{(r)}(\omega) = \int E_x^{(r)}(\tau + t)e^{i\omega t}\,dt$, assumes the form

$$E_x^{(r)}(\omega) = -\Gamma_0\int_0^\infty e^{i(\omega-\omega_0+i\Gamma')t + ik_0[u_z(\tau)+u(\tau+t)]}\,dt, \tag{10}$$

where $k_0 = \omega_0/c$ and we assumed additionally that the resonance of the layer is well resolved, $\Gamma' \ll \omega_0$. A similar consideration for the transmitted wave gives the spectrum

$$E_x^{(t)}(\omega) = 1 - \Gamma_0\int_0^\infty e^{i(\omega-\omega_0+i\Gamma')t + ik_0[u_z(\tau)-u(\tau+t)]}\,dt, \tag{11}$$

where the unity term stems from the spectrum of the incident light pulse. The reflected and transmitted power spectra read $R(\omega) = |E_x^{(r)}(\omega)|^2$ and $T(\omega) = |E_x^{(t)}(\omega)|^2$.

It is instructive to consider also the reflection and transmission spectra averaged over the probe arrival time τ. Performing the averaging in Eqs. (10) and (11), we get

$$\overline{R}(\omega) = \frac{\Gamma_0^2}{\Gamma'}C(\omega - \omega_0), \tag{12}$$

$$\overline{T}(\omega) = 1 - \frac{\Gamma_0(\Gamma_0 + 2\Gamma)}{\Gamma'}C(\omega_0 - \omega), \tag{13}$$

where

$$C(\omega) = \mathrm{Re}\int_0^\infty C(t)e^{i\omega t - \Gamma' t}dt, \tag{14}$$

$$C(t) = \langle e^{ik_0[u_z(\tau+t)-u_z(\tau)]}\rangle_\tau, \tag{15}$$

the angular brackets denote averaging over τ, and we recall that $\Gamma' = \Gamma + \Gamma_0$. In the absence of nonradiative decay, $\Gamma = 0$, the conservation law

$$\overline{R}(\omega) + \overline{T}(2\omega_0 - \omega) = 1 \tag{16}$$

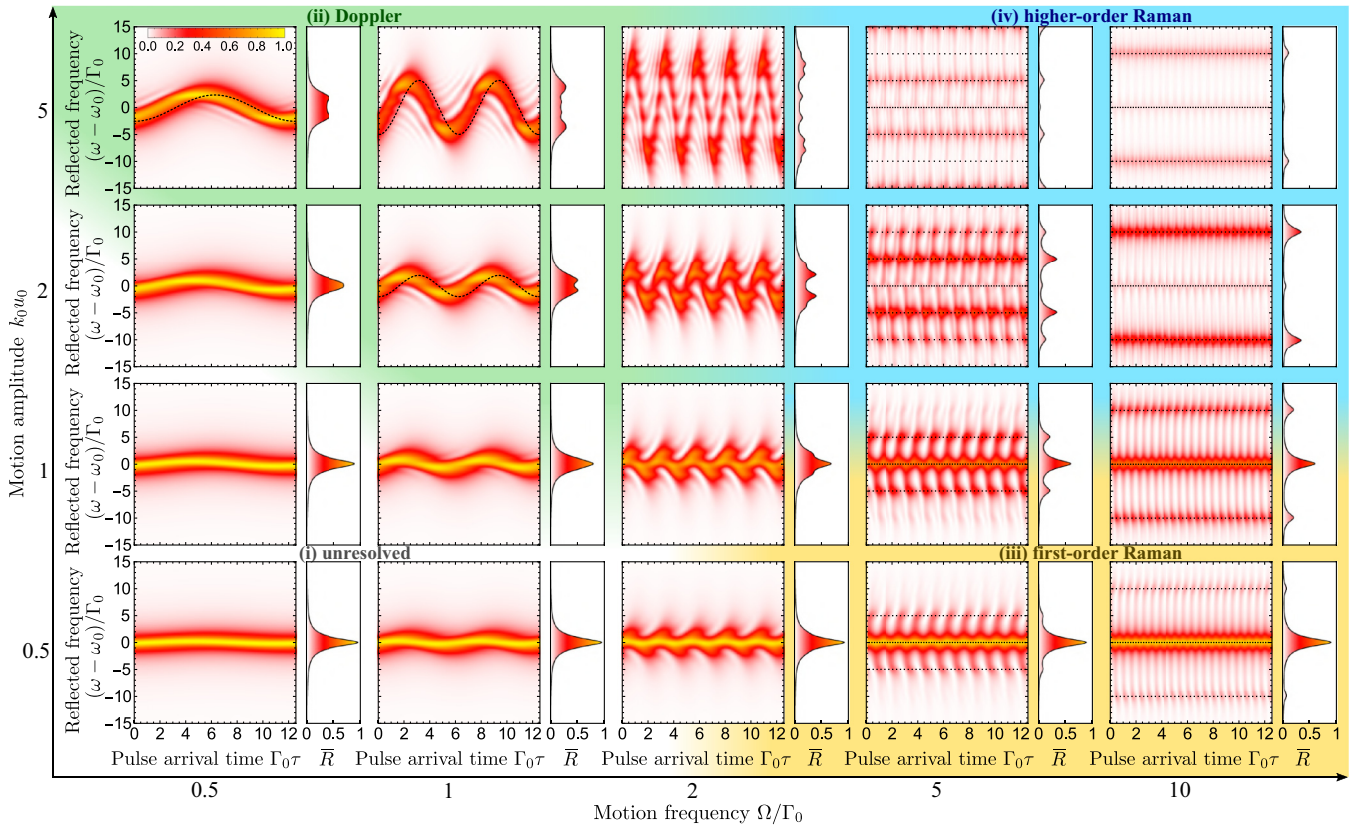

FIG. 2. The reflected light spectra after excitation of the resonant layer periodically moving in space with a short pulse. The plots are calculated for various motion frequencies and amplitudes, revealing the crossover between different scattering regimes, indicated by the background color. The left panels show the color plots of the spectra as a function of pulse arrival time τ. The right panels show the τ-averaged spectra. The nonradiative resonance broadening is supposed to be absent, $\Gamma = 0$.

is fulfilled, i.e., the sum of the reflected spectral power taken at the frequency shifted up by the Doppler effect and transmitted spectral power taken at the frequency shifted down, or vice versa, is equal to the spectral power of the incident pulse. If the motion of the layer is invariant under time-reversal symmetry, $C(t) = C(-t)$, then $C(t)$ is real and $C(\omega) = C(-\omega)$. In such a case, both the reflected and transmitted power spectra are symmetric with respect to the resonance frequency ω_0, while the conservation law assumes a simpler form $\overline{R}(\omega) + \overline{T}(\omega) = 1$. The total reflected power $\int \overline{R}(\omega)d\omega/(2\pi) = \Gamma_0^2/\Gamma'$ does not depend on the specifics of layer motion, that only redistributes the power over the spectrum.

A. Periodic layer motion

First, we consider the case of the periodic layer motion described by $u_z(t) = u_0 \sin \Omega t$. Shown in Fig. 2 are the color plots of the reflected light spectra $R(\omega)$ depending on the pulse arrival time τ and calculated for various motion amplitudes and frequencies. The graphs on the right present the τ-averaged spectra $\overline{R}(\omega)$. We distinguish several regimes indicated by the color fill.

When $\Omega \ll \Gamma'$, the pulse is reflected at a timescale smaller than the motion period. Therefore, its spectral conversion is governed by the Doppler effect in the corresponding time moment. If the Doppler shift is small, $k_0u_0\Omega \ll \Gamma'$ [regime (i), white area], the effect is smeared by resonance broadening. If $k_0u_0\Omega \gg \Gamma'$ [regime (ii), green area], the maximum of the reflected spectrum shifts strongly with the pulse arrival time τ following the layer velocity, $\omega_0[1 - (\Omega u_0/c)\cos \Omega t]$, indicated by the dashed curve, with a retardation on the order of $1/\Gamma'$.

As the motion frequency is increased, $\Omega \sim \Gamma'$, the sidebands start to appear around the central peak that still follows the cosine dependence of the Doppler shift [10]. The case $\Omega \gg \Gamma'$ corresponds to the well-resolved Raman sidebands while the cosine dependence of the Doppler shift is fragmentized. The τ-averaged spectra $\overline{R}(\omega)$ is conveniently presented as the sum of Lorentzians at the sideband frequencies,

$$\overline{R}(\omega) = \sum_{n=-\infty}^{\infty} J_n^2(k_0u_0)\frac{\Gamma_0^2}{(\omega - n\Omega)^2 + \Gamma'^2}, \qquad (17)$$

where J_n is the Bessel function of the first kind. When the Raman scattering probability is weak, $k_0u_0 \ll 1$ [regime (iii), yellow area], only the first-order scattering sideband is revealed (see dashed lines indicating the sidebands at $\omega_0 \pm \Omega$). If $k_0u_0 \gtrsim 1$ [regime (iv), blue area], the sidebands of higher order begin to appear, while the amplitude at the initial frequency ω_0 gets suppressed, in accordance with Eq. (17). We note that Eq. (17) is valid in all scattering regimes. While the peaks corresponding to different sidebands are well resolved in the regimes of the Raman effect (iii) and (iv), they overlap in the regime of the Doppler effect (ii). Then, the

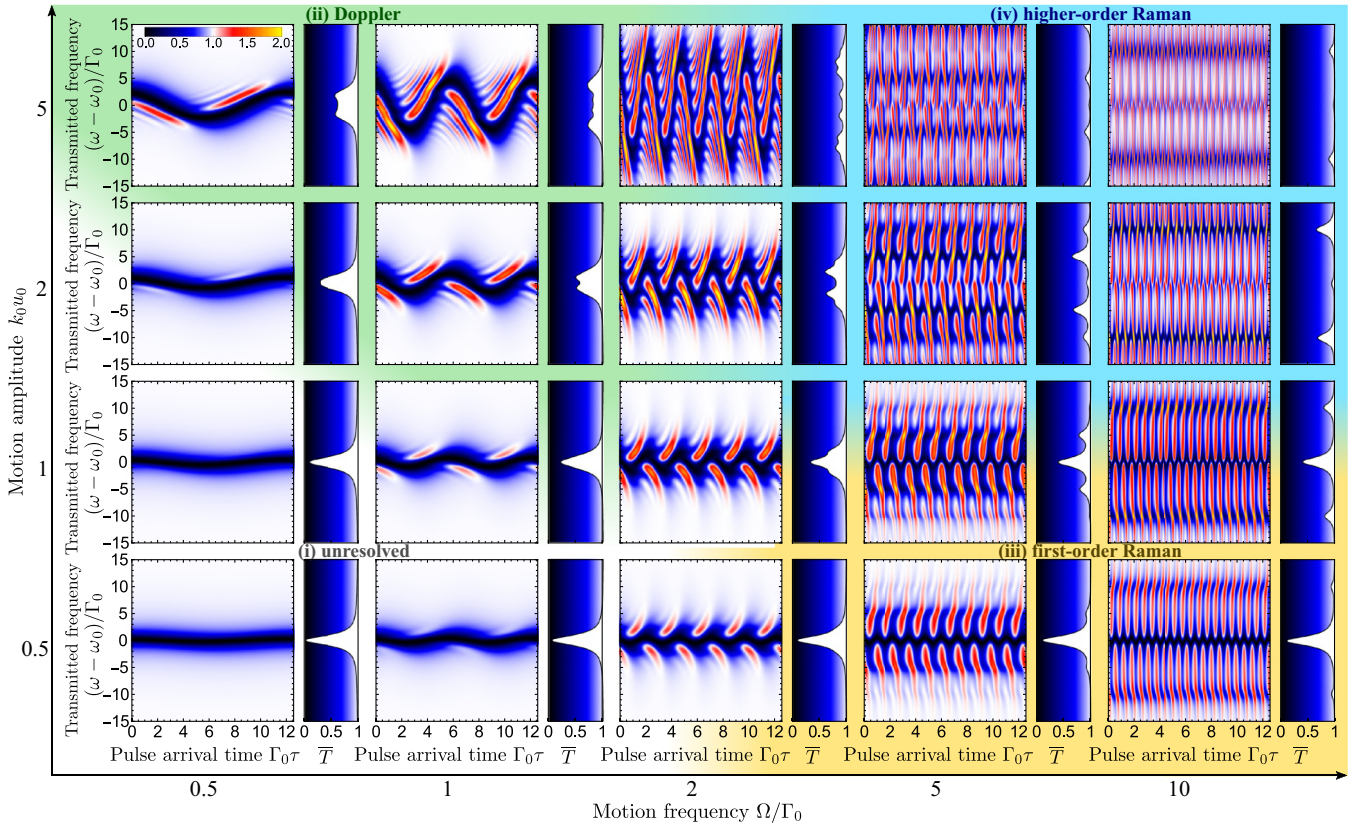

FIG. 3. The transmitted light spectra after excitation of the resonant layer periodically moving in space with a short pulse. Background colors indicate different scattering regimes. The left panels show the color plots of the spectra depending on the pulse arrival time τ. The right panels show the τ-averaged spectra. The nonradiative resonance broadening is supposed to be absent, $\Gamma = 0$.

spectrum assumes a non-Lorentzian shape corresponding to the time-averaged Doppler shift.

Figure 3 shows the color plots for the transmitted light spectra. The Doppler shift has opposite signs for transmitted and reflected light [cf. the spectra evolution in regime (ii) in Figs. 2 and 3]. The other difference of the transmitted light spectra from that of the reflected light is that the transmitted light is the result of interference between the initial pulse [first term in Eq. (11)] and the scattered light [second term in Eq. (11)]. Depending on the phase of the scattered light, the interference can be both constructive and destructive. As a result, the spectral intensity of the transmitted pulse can be both greater or smaller than that of the incident pulse [10], which is encoded by red and blue colors in Fig. 3, respectively.

B. Stochastic layer motion

Now we turn to the case when the layer displacement $u_z(t)$ is a stochastic function of time. The averaged reflection and transmission spectra are still given by Eqs. (12)–(15), where the averaging over τ should be replaced by averaging over the realizations of the function $u_z(t)$.

We assume that the displacement $u(t)$ has a Gaussian probability distribution. To evaluate the spectra, we rewrite Eq. (15) as $C(t) = \langle e^{i(\omega_0/c)\int_0^t \dot{u}_z(t')dt'}\rangle$. Next, we expand the exponent into the series, use the Wick's theorem, and obtain

$$C(t) = e^{(k_0^2/2)\int_0^t\int_0^t \ddot{K}(t'-t'')dt'dt''}, \tag{18}$$

where $K(t) = \langle u_z(0)u_z(t)\rangle$ is the correlation function of the layer displacement. Performing integration in Eq. (18), we finally get

$$C(t) = e^{k_0^2[K(t)-K(0)]}. \tag{19}$$

As an example, we consider the case when the layer motion corresponds to a harmonic oscillator driven by a stochastic force with a white-noise spectrum. The Fourier component of the displacement correlation function is $K(\omega) \propto 1/[\omega^2 - (\Omega + i\gamma)^2]$, which yields

$$K(t) = \overline{u^2}\left(\cos\Omega t + \frac{\gamma}{\Omega}\sin\Omega|t|\right)e^{-\gamma|t|}, \tag{20}$$

where Ω is the eigenfrequency of the oscillator, γ is its damping rate, and $\overline{u^2}$ is the variance of the layer displacement. We suppose that $\gamma \ll \Omega, \Gamma'$ and obtain

$$C(\omega) = \mathrm{Re}\int_0^\infty e^{k_0^2\overline{u^2}(\cos\Omega t-1)+i\omega t-\Gamma' t}dt. \tag{21}$$

Similarly to the case of periodic motion, the reflected pulse power spectra can be decomposed into a sum of Lorentzians centered at the Raman sideband frequencies,

$$\overline{R}(\omega) = e^{-k_0^2\overline{u^2}}\sum_{n=-\infty}^{\infty} I_n\left(k_0^2\overline{u^2}\right)\frac{\Gamma_0^2}{(\omega-n\Omega)^2+\Gamma'^2}, \tag{22}$$

where I_n is the modified Bessel function of the first kind. Resolved sidebands are realized in the regime of Raman

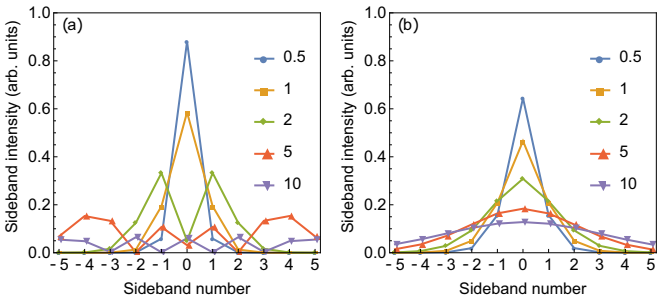

FIG. 4. The intensity of the Raman sidebands in the spectra of the pulse reflected from a resonant layer that moves (a) periodically as $u(t) = u_0 \sin \Omega t$ and (b) randomly with the correlation function $\langle u(0)u(t)\rangle = \overline{u^2}\cos\Omega t$. Points correspond to different motion amplitudes, characterized by parameters k_0u_0 and $k_0\sqrt{\overline{u^2}}$, for the case of periodic and random motion, respectively. Lines are a guide for the eye.

scattering, $\Omega \gg \Gamma'$; if $\Omega \ll \Gamma'$, the spectrum assumes the form of the averaged Doppler shift. Equation (22) can be obtained by averaging the result for periodic motion Eq. (17) over the Gaussian distribution of motion amplitudes, $\int_0^\infty \overline{R}(\omega)u_0\, e^{-u_0^2/(2\overline{u^2})}/\sqrt{\overline{u^2}}\, du_0$.

Figure 4 shows the intensities of the sidebands for different amplitudes of layer motion. Figures 4(a) and 4(b) correspond to the cases of periodic and stochastic layer motion, respectively. For periodic harmonic layer motion, in Fig. 4(a) the sideband intensity oscillates with the sideband number. For large motion amplitudes, the most intensive sideband is that with the number $\propto k_0u_0$. In contrast, in the case of stochastic layer motion shown in Fig. 4(b), the intensities of the sidebands decay monotonously with the sideband number.

IV. TIME-MODULATED RESONANCE

The essence of the considered Doppler-Raman crossover is the periodic modulation of the layer resonant frequency due to the Doppler shift. However, such modulation can be also realized directly. Generally, a deformation of the layer can lead to a shift of its resonance. This effect is especially strong in semiconductors, where the deformation potential mechanism leads to a strong shift of the exciton energy by $\delta\omega_x = \Xi\zeta$, where ζ is the deformation and $\Xi \sim 10$ eV [6,21].

Consider the quantum well with the exciton resonance frequency changing in time as

$$\omega_r(t) = \omega_x + \delta\omega_x \cos\Omega t \tag{23}$$

due to the effect of an acoustic wave. The evolution of the exciton dipole polarization of the quantum well is described by the modified version of Eq. (6) with $u_z = 0$ and ω_0 replaced with $\omega_r(t)$,

$$\ddot{P}_x + \omega_r(t)^2 P_x + 2\Gamma'\dot{P}_x = -\frac{\Gamma_0}{\pi}\frac{\partial A_0}{\partial t}(0,t). \tag{24}$$

We again suppose that the frequency shifts are small $\delta\omega_x, \Omega \ll \omega_x$ and use the Wentzel-Kramers-Brillouin approximation to solve Eq. (24),

$$P_x(t) = \frac{\Gamma_0\theta(t-\tau)}{\pi\sqrt{\omega_r(t)\omega_r(\tau)}}\sin\left[\int_\tau^t \omega_r(t')dt'\right]e^{-\Gamma'(t-\tau)}. \tag{25}$$

Then, the reflected light spectrum at the frequencies close to ω_x is given by

$$E_r(\omega) = -\Gamma_0\int_0^\infty e^{i(\omega+i\Gamma')t - i\int_\tau^{\tau+t}\omega_r(t')dt'}\,dt, \tag{26}$$

while the transmitted spectrum is $E_t(\omega) = 1 + E_r(\omega)$. In the absence of nonradiative damping, $\Gamma = 0$, the conservation law has the form $\overline{R}(\omega) + \overline{T}(\omega) = 1$.

The reflected pulse spectra for the cases of a trembling layer and a layer with oscillating resonance frequency, Eqs. (10) and (26) match (up to a certain phase) if one takes $\delta\omega_x(t) = \omega_0\dot{u}(t)$. That is exactly the condition of the Doppler shift for backscattered light being emulated by the direct modification of the resonance frequency. Similarly, the transmitted light spectra match if $\delta\omega_x(t) = -\omega_0\dot{u}(t)$.

V. CONCLUSION

To conclude, we have developed a theory of light interaction with moving resonant layers. The scattering of short pulses by layers oscillating in space was considered. Our calculation demonstrates that when the motion frequency is small as compared to the resonance width, the spectrum of the reflected pulse features a peak at the frequency that changes in time, in accordance with the Doppler effect. In the opposite case of high layer motion frequency, the reflected spectrum comprises several Raman sidebands shifted by multiples of the mechanical frequency. The intensities of the sidebands are determined by the correlation function of layer displacement. Both effects, as well as the crossover between them, can be emulated by use of the quantum well, where the exciton resonance frequency is modulated by strain.

ACKNOWLEDGMENTS

This work was supported by the Russian Science Foundation (Project No. 20-42-04405). A.V.P. acknowledges the partial support from the Russian President Grant No. MK-599.2019.2 and the RFBR Grant No. 20-32-70048.

APPENDIX: DERIVATION OF THE ACTION

Here, we derive the Lagrangian describing the interaction between the electromagnetic field and the moving dipole $\boldsymbol{P}(t)$. The dipole position at time t is given by $\boldsymbol{r} = \boldsymbol{u}(t)$. We start from the action of a particle with charge e in electromagnetic field [22],

$$S = e\int \boldsymbol{A}[\boldsymbol{r}(t),t]\dot{\boldsymbol{r}}(t)dt. \tag{A1}$$

The dipole $\boldsymbol{P}(t)$ can be represented by two charges, $+e$ and $-e$, located at coordinates $\boldsymbol{r} = \boldsymbol{u}(t) + \boldsymbol{P}(t)/2e$ and $\boldsymbol{r} = \boldsymbol{u}(t) - \boldsymbol{P}(t)/2e$, respectively. Then, using Eq. (A1) and considering the limit $e \to \infty$, we obtain the action

$$S = \int[(\boldsymbol{P}\cdot\nabla)\boldsymbol{A}(\boldsymbol{u},t) + \boldsymbol{A}(\boldsymbol{u},t)\cdot\dot{\boldsymbol{P}}]dt. \tag{A2}$$

Finally, we perform integration by parts and get

$$S = \int \boldsymbol{P} \cdot [\boldsymbol{E}(\boldsymbol{u}, t) + \dot{\boldsymbol{u}} \times \boldsymbol{B}(\boldsymbol{u}, t)]dt. \tag{A3}$$

Note that here $\boldsymbol{P}$ is the dipole in the reference frame at rest. However, in the relevant case of $\boldsymbol{u} \perp \boldsymbol{P}$, it coincides with the dipole in the moving reference frame.

[1] R. W. Boyd, *Nonlinear Optics* (Academic Press, New York, 2003).

[2] L. Fan, C.-L. Zou, M. Poot, R. Cheng, X. Guo, X. Han, and H. X. Tang, Nat. Photon. **10**, 766 (2016).

[3] S. F. Preble, Q. Xu, and M. Lipson, Nat. Photon. **1**, 293 (2007).

[4] C. B. Scruby and L. E. Drain, *Laser Ultrasonics: Techniques and Applications* (Hilger, Bristol, UK, 1990).

[5] E. Kuramochi and M. Notomi, Nat. Photon. **10**, 752 (2016).

[6] A. A. Demenev, D. D. Yaremkevich, A. V. Scherbakov, S. M. Kukhtaruk, S. S. Gavrilov, D. R. Yakovlev, V. D. Kulakovskii, and M. Bayer, Phys. Rev. B **100**, 100301(R) (2019).

[7] D. J. Farmer, A. V. Akimov, N. A. Gippius, J. Bailey, J. S. Sharp, and A. J. Kent, Opt. Express **22**, 15218 (2014).

[8] C. Brüggemann, A. V. Akimov, A. V. Scherbakov, M. Bombeck, C. Schneider, S. Höfling, A. Forchel, D. R. Yakovlev, and M. Bayer, Nat. Photon. **6**, 30 (2011).

[9] B. Jusserand, A. N. Poddubny, A. V. Poshakinskiy, A. Fainstein, and A. Lemaitre, Phys. Rev. Lett. **115**, 267402 (2015).

[10] T. Berstermann, A. V. Scherbakov, A. V. Akimov, D. R. Yakovlev, N. A. Gippius, B. A. Glavin, I. Sagnes, J. Bloch, and M. Bayer, Phys. Rev. B **80**, 075301 (2009).

[11] T. Berstermann, C. Brüggemann, A. V. Akimov, M. Bombeck, D. R. Yakovlev, N. A. Gippius, A. V. Scherbakov, I. Sagnes, J. Bloch, and M. Bayer, Phys. Rev. B **86**, 195306 (2012).

[12] A. V. Poshakinskiy and A. N. Poddubny, Phys. Rev. X **9**, 011008 (2019).

[13] A. V. Poshakinskiy and A. N. Poddubny, Phys. Rev. Lett. **118**, 156801 (2017).

[14] C. Zhu, L. Dong, and H. Pu, Phys. Rev. A **94**, 053621 (2016).

[15] C. Zhu, L. Dong, and H. Pu, J. Phys. B **49**, 145301 (2016).

[16] L. C. Andreani, G. Panzarini, A. V. Kavokin, and M. R. Vladimirova, Phys. Rev. B **57**, 4670 (1998).

[17] D. Ammerlahn, J. Kuhl, B. Grote, S. W. Koch, G. Khitrova, and H. Gibbs, Phys. Rev. B **62**, 7350 (2000).

[18] A. V. Poshakinskiy, A. N. Poddubny, and S. A. Tarasenko, Phys. Rev. B **86**, 205304 (2012).

[19] M. Aspelmeyer, T. J. Kippenberg, and F. Marquardt, Rev. Mod. Phys. **86**, 1391 (2014).

[20] S. V. Bulanov, T. Z. Esirkepov, M. Kando, A. S. Pirozhkov, and N. N. Rosanov, Phys. Usp. **56**, 429 (2013).

[21] P. Yu and M. Cardona, *Fundamentals of Semiconductors: Physics and Materials Properties*, Graduate Texts in Physics (Springer, Berlin, 2010).

[22] L. Landau and E. Lifshitz, *The Classical Theory of Fields*, 4th ed., Course of Theoretical Physics Vol. 2 (Elsevier, Amsterdam, 2009).